Journal of Thermal Analysis and Calorimetry (2019) 136:1551–1561
https://doi.org/10.1007/s10973-018-7815-5

# Microencapsulated oleic–capric acid/hexadecane mixture as phase change material for thermal energy storage

Mehmet Selçuk Mert[1] · Hatice Hande Mert[2] · Merve Sert[1]

Received: 19 April 2018 / Accepted: 7 October 2018 / Published online: 17 October 2018


## Abstract

Thermal energy storage systems provide efficiency in order to have better utilization of energy sources while protecting the environment. Thermal energy storage can be classified as sensible and latent heat storage. The storage of latent heat allows a greater density of energy storage with a narrow temperature range during phase change. Phase change materials (PCMs) are important novel materials, which are used as the storage of thermal energy as latent heat, and can provide utilization of waste heat energy. In this study, the capric acid and oleic acid mixture containing hexadecane were encapsulated as the core with styrene–divinylbenzene copolymer shell by emulsion polymerization technique. Thermal properties of fatty acid microcapsules were characterized by differential scanning calorimetry and thermogravimetric analysis and also their morphology and structure were examined by scanning electron microscopy, polarized optical microscopy and Fourier transform infrared spectroscopy (FT-IR), respectively. The heat storage property of microencapsulated PCM was tested in a horizontal air flow channel system equipped with a flat heating plate, air fan and air flow sensors. The microencapsulated PCM was prepared successfully, and results of the analysis presented that this material is promising candidate for potential heating and cooling system applications.

**Keywords** Energy · Phase change material · Encapsulation · Thermal energy storage

## Introduction

The phase change materials (PCMs) are a promising choice for thermal energy storage. The latent heat energy storage can be achieved via absorbing heat and releasing heat at a certain temperature range by using phase change materials (PCMs). These materials, which have high thermal storage capacity, can be classified into three groups as organic, inorganic and eutectic compounds. The organic phase change materials are composed mainly of fatty acids and paraffins. Fatty acids have some advantages with respect to the other materials, namely high thermal storage capacity, small volume change during phase change, chemically stable, non-corrosive and not involve phase segregation [1–4]. On the other hand, paraffins exhibit large volume changes during phase change, and thermal conductivities are low; thus, they have to be encapsulated for using on thermal energy storage systems. The volume of the phase change material during the phase change can be kept and also the thermal conductivity of the paraffins can be increased by the encapsulation process. Among the different encapsulation methods, the emulsion polymerization method has some advantages compared to the other methods. The polymerization temperature is low and is in contrast; the polymerization rate is high. Furthermore, the production process is easy, and it is inexpensive to work with water. *n*-Heptadecane, *n*-hexadecane and *n*-octadecane can be given as the examples of the paraffins used in the preparation of the phase change materials by emulsion polymerization method [5–8]. Paraffins can also be used for forming different paraffin mixtures in order to the preparation of phase change materials.

In recent years, composite PCMs have been drawing more attention due to improving of thermal conductivity of material. Especially, graphite is one of the most preferring

✉ Mehmet Selçuk Mert
msmert@yalova.edu.tr

[1] Energy Systems Engineering Department, Yalova University, 77200 Yalova, Turkey

[2] Chemical and Process Engineering Department, Yalova University, 77200 Yalova, Turkey

additives with advantages such as porous structure, perfect thermal conduction performance and great adsorption properties [9]. Furthermore, expanded graphite has been used for preparation of form-stable composite PCMs as a multi-porous supporting matrix [10]. The shape-stabilized thermal energy storage materials could also be prepared by using inorganic shells such as $TiO_2$ [11] or adding carbon nanotubes (CNTs) as the supporting matrix [12]. Alkan and Sarı synthesized fatty acids as form-stable PCM using PMMA which acts as supporting material by solution casting method. It has been stated that while the fatty acids are heated over the melting point, the prepared shape-stable SA/PMMA, PA/PMMA, MA/PMMA and LA/PMMA (80% mass) PCMs kept their shape [13]. Moreover, Sarı et al. studied SA/SMA, MA/SMA, PA/SMA and LA/SMA composites of fatty acids using the SMA, which acts as a shell material. The encapsulation ratio of fatty acids was as much as 85 mass/%, and when the temperature of the composite PCM was over the melting point of the fatty acid, no leakage was observed. DSC results show that composite PCMs have suitable phase change temperatures and satisfying latent heat storage capacities for solar energy storage with wallboard and plasterboard heat and underfloor area heating of buildings [14].

There are also numerous patents that report the preparation and characterization of PCMs. Bellemare [15] filed a patent reporting five methods to improve PCMs electrical and thermal conductivity via applying a conductive layer on the encapsulated PCM. Among them, electroless deposition method found to be useful for applying the conductive layer. Furthermore, coating of silver layer on the PCM has significantly enhanced the thermal and electrical conductivity. In another work, Zhang et al. [16] proposed the use of the mixture of organic and inorganic materials as a shell to provide enhanced properties for the shell. They stated that, utilizing the structural flexibility and easier processing of organic materials and benefiting from the stability, flame retardancy, strength and conductivity of inorganic materials give an opportunity to prepare a desired shell material. In another patent, Hart and Work [17] reported that decabromodiphenyl oxide, octabromophenyl oxide, antimony oxide etc. can be added to the encapsulated PCMs as a flame retardant. Hatfield [18] has performed the encapsulation of polyethylene glycol 8000 into polyurethane–urea shell material. It was found that elastomeric shell material met the volume change during the phase change process. Additionally, it was observed that the latent heat of fusion reduced in a small amount with the encapsulation of the PCM.

The phase change materials which were obtained by preparing different combinations of fatty acids and paraffins have found a wide study range in the literature. Among them, the most frequently investigated fatty acids are capric acid (CA), lauric acid (LA), myristic acid (MA), palmitic acid (PA), oleic acid (OA) and stearic acid (SA) [19]. It is important for the application in practical engineering systems to determine the thermophysical properties of pure fatty acids and fatty acid mixtures via investigating thermal reliability and clarifying the chemical structures. For this aim, thermal properties, thermal stability, chemical structure and morphological properties can be determined by differential scanning calorimetry (DSC), Fourier transform infrared spectrophotometer (FT-IR), thermogravimetric analyzer (TG) and scanning electron microscope (SEM) analyzes. In the previous studies, in addition to pure fatty acids, mixtures of lauric–stearic acid (LA–SA), myristic–palmitic acid (MA–PA), palmitic–steatric acid (PA–SA), lauric–palmitic acid (LA–PA), myristic–stearic acid (MA–SA) and capric–palmitic acid (CA–PA), as well as the triple mixtures of the capric–lauric–palmitic acid (CA–LA–PA), capric–palmitic–stearic acid (CA–PA–SA), lauric–myristic–palmitic acid (LA–MA–PA), lauric–myristic–stearic acid (LA–MA–SA), lauric–palmitic–stearic acid (LA–PA–SA) and myristic–palmitic–stearic acid (MA–PA–SA) have also been investigated [19–31]. The thermal properties of some mixtures are given in Table 1.

In spite of the novelties of studies mentioned above, the works generally were based on using paraffins or fatty acids separately as pure or mixtures in itself for preparing latent heat storage material. However, to the best of our knowledge, there is no available work in the literature about the microencapsulation of mixtures of fatty acids in the presence of paraffin which takes the role both as a phase change material and a co-emulsifier in the oil/water emulsion system. In this regard, the first aim of this study is the preparation of microencapsulated phase change material, which was composed of fatty acid mixtures accompanied by paraffin via emulsion polymerization and the performing of morphological, chemical and thermal characterizations of it. The microencapsulated PCM was composed of the oleic acid–capric acid–hexadecane as the core material and styrene–divinylbenzene polymer as the shell. As known from the literature [32, 33], long-chain alkanes or alcohols can be added to an emulsion system consisted of water, monomer and surfactant in order to form relatively stable droplets during the polymerization and retard the destabilization of droplets efficiently by Ostwald ripening. In this regard, it is intended that *n*-hexadecane as a long-chain alkane used in the oil/water emulsion system was not only as a phase change material but also contributed as a co-emulsifier with its unique structure for providing the stabilization of the emulsion system. The thermal, morphological and structural properties of microencapsulated PCM were determined by DSC, TG, SEM, POM and FT-IR analyses, respectively. Moreover, the second aim of this work was demonstrating

**Table 1** Thermal properties of fatty acid and fatty acid mixtures

| Material | Mass ratio | Melting point range/°C | Latent heat of fusion range/kJ $kg^{-1}$ | Freezing point range/°C | Latent heat of crystallization range/kJ $kg^{-1}$ | References |
|---|---|---|---|---|---|---|
| CA | 100 | 29.62–32.14 | 139.77–156.40 | 25.57–32.53 | 140.12–154.24 | [19] |
| LA | 100 | 42.14–44.33 | 175.8–217.29 | 39.78–42.20 | 180.51–194.23 | [19] |
| MA | 100 | 51.5–58 | 178.14–210.7 | 51.74–52.49 | 181.63–184.9 | [19] |
| PA | 100 | 58.9–65.5 | 185.4–233.24 | 58.23–60.38 | 205.39–237.11 | [19] |
| SA | 100 | 53.8–70.9 | 159.3–258.98 | 37.06–66.36 | 177.80–263.32 | [19] |
| CA–LA | 67:33 | 22.81 | 154.16 | 16.43 | 125.2 | [6, 19] |
| CA–MA | 74:26 | 22.16 | 154.83 | 21.18 | 156.42 | [22] |
| CA–PA | 76.5:23.5 | 21.85 | 171.22 | 22.15 | 150.29 | [23] |
| CA–SA | 83:17 | 25.39 | 188.15 | 25.2 | 184.11 | [19] |
| LA–MA | 64:36 | 32.2–36.2 | 168.8 | – | – | [25] |
| LA–PA | 67:33 | 34.1–36.1 | 168.4 | – | – | [19, 25] |
| LA–SA | 75.5:24.5 | 37 | 182.7 | 32.25 | 166.5 | [19, 24]. |
| MA–SA | 77.42:22.58 | 46.41 | 180.6 | 42.09 | 177.3 | [19] |
| MA–PA | 57:43 | 42–42.9 | 169.9 | – | – | [24] |
| PA–SA | 62.99:37.01 | 56.16 | 204.7 | 52.43 | 204.2 | [20] |
| CA–LA–MA | 56.39:26.72:16.89 | 18.72 | 131.4 | 11.14 | 129.7 | [20] |
| CA–LA–PA | 63.37:31.56:5.07 | 20.75 | 134.0 | 11.95 | 132.5 | [20] |
| CA–LA–SA | 65.32:32.54:2.14 | 22.80 | 132.5 | 13.10 | 129.7 | [20] |
| CA–MA–PA | 71.82:18.86:9.32 | 22.31 | 136.8 | 12.83 | 132.6 | [20] |
| CA–MA–SA | 72.65:21.17:6.18 | 24.04 | 145.9 | 13.63 | 143.1 | [20] |
| CA–PA–SA | 79.3:14.7:6.0 | 18.9 | 147.2 | 16.73 | 142.3 | [29] |
| LA–MA–PA | 55.24:29.74:15.02 | 31.41 | 145.8 | – | – | [31] |
| LA–MA–SA | 55.8:32.8:11.4 | 29.29 | 140.9 | 28.38 | 137.2 | [30] |
| LA–PA–SA | 72.26:20.97:6.77 | 36.79 | 159.0 | 28.46 | 159.5 | [20] |
| MA–SA–PA | 52.5:17.2:30.3 | 49.23 | 170.3 | 40.42 | 168.7 | [20] |
| MA–PA–SA | 52.2:29.4:18.4 | 41.72 | 163.5 | 42.38 | 159.8 | [27] |

its potential for low-temperature heating and cooling systems by testing the heat storage property of manufactured microencapsulated PCM by using a laboratory scale experimental system.

## Materials and methods

### Materials

2,2′-Azobisisobutyronitrile, AIBN (initiator, 98%) was purchased from Aldrich Chemistry and recrystallized in the ethanol. Styrene (St) (monomer, Merck, Darmstadt, Germany), divinylbenzene (DVB) (cross-linking agent, 80%, Aldrich Chemistry, Steinheim, Germany), cetyl trimethylammonium bromide (CTAB) (cationic surfactant, 98% Sigma), oleic acid (OA) (fatty acid, 90% Sigma) and capric acid (CA) (fatty acid, 98% Sigma), *n*-hexadecane (HD) (paraffin, Merck, Darmstadt, Germany) were used as received. The chemical properties of the materials used are given in Table 2.

## Experimental

### Preparation of microencapsulated PCMs

OA–CA–HD/St–DVB microcapsules were prepared by emulsion polymerization according to the procedure described below. The volumetric core–shell ratio was kept constant to be 1:1 during the encapsulation process. The water phase was composed of CTAB and deionized water. The concentration of the CTAB was fixed to 50 mmol $L^{-1}$, and it was mixed with a magnetic stirrer for 10 min at room temperature.

The oil phase was prepared by mixing the St and DVB monomers, the mixture of OA, CA and HD and the AIBN initiator (0.1 g) at room temperature for 10 min. Then, the water phase was added drop by drop to the oil phase and stirring was continued for 1 h with a mechanical stirrer. The obtained oil/water emulsion was polymerized at 70 °C for 6 h in a system equipped with a reflux condenser. At the end of the reaction period, the product obtained is cooled to room temperature and precipitated in ethanol. The

**Table 2** Chemical properties of materials

| Material | Formula | Molecular mass/g $mol^{-1}$ | Boiling point/°C | Melting point/°C |
|---|---|---|---|---|
| OA | $C_{18}H_{34}O_2$ | 282.46 | 194 | 13–14 |
| CA | $C_{10}H_{20}O_2$ | 172.26 | 268 | 27–32 |
| HD | $C_{16}H_{34}$ | 226.44 | 287 | 18 |
| St | $C_8H_8$ | 104.15 | 145 | − 31 |
| DVB | $C_{10}H_{10}$ | 130.20 | 195 | − 67 |

**Table 3** The composition of microencapsulated PCMs prepared by emulsion polymerization method

| Core content | Volume percent/%v/v | Shell content | Volume percent/%v/v |
|---|---|---|---|
| OA | 25 | St | 90 |
| CA | 25 | DVB | 10 |
| HD | 50 | | |

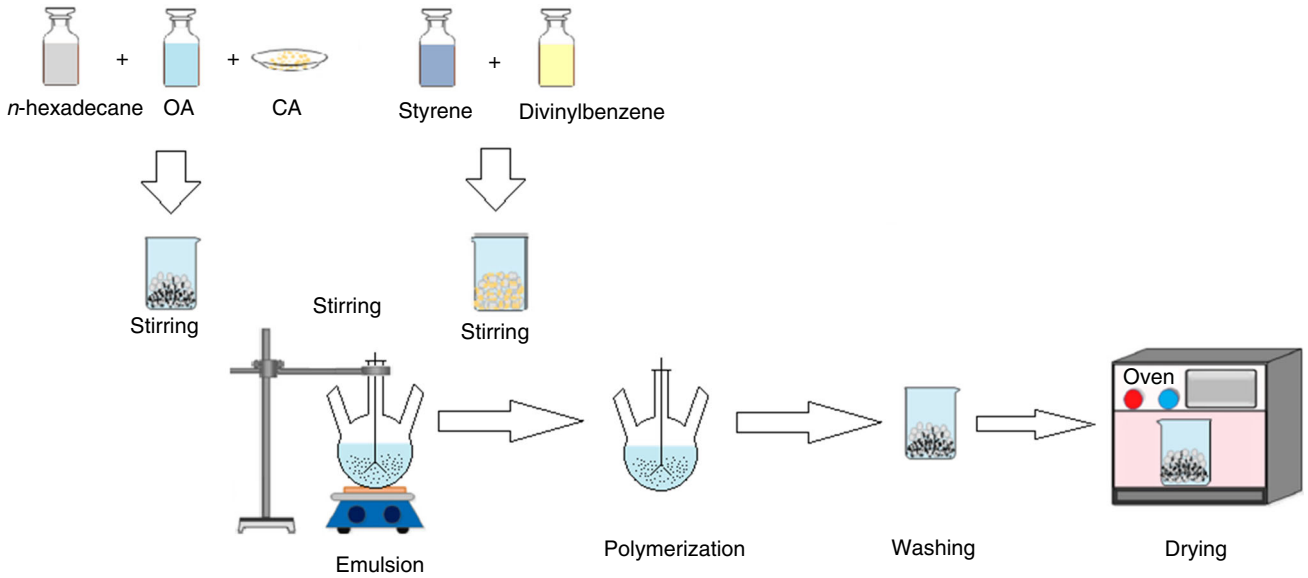


**Fig. 1** Schematic representation of the encapsulation process

precipitated product was filtered and washed with deionized water and dried at 40 °C in a vacuum oven for 24 h. The composition of the microcapsules is given in Table 3. The preparation process of microencapsulated PCM and the reaction scheme of poly(styrene-co-divinylbenzene) shells are shown in Figs. 1 and 2, respectively.

### Characterization of microencapsulated PCMs

The morphological characteristics of the microencapsulated PCM and the empty shell material were examined by scanning electron microscope (SEM) analysis (FEI Inc. Inspect S50 SEM-EDAX) and polarized optical microscope (POM) (Leica Polarizing Microscope). The size distribution of the microcapsules was determined by using the data from the SEM image through CoralDRAW X8 program. FT-IR spectra of the encapsulated PCM mixture, pure OA–CA–HD mixture and St–DVB copolymer shell of were obtained using FT-IR spectrophotometer (Perkin Elmer, Spectrum 100) at a wavelength of 650–4000 $cm^{-1}$ at room temperature. The thermogravimetric analysis (TG) of the materials was performed with a thermal analyzer (Seiko TG/DTA 6300 thermal analysis system instrument, Seiko Instruments, Tokyo, Japan) at a heating rate of 10 °C $min^{-1}$ under nitrogen atmosphere. Differential scanning calorimetry (DSC) measurements were performed with DSC 7020 (HITACHI) under nitrogen atmosphere and at 10 °C $min^{-1}$ heating rate. The melting temperature ($T_m$), crystallizing temperature ($T_c$), latent heat of fusion ($\Delta H_f$) and latent heat of crystallization ($\Delta H_c$) of the microencapsulated PCM and the pure PCM mixture were determined by DSC measurements. The encapsulation rate of the PCM mixture was calculated using the following formula, depending on the measured enthalpy values [34]:

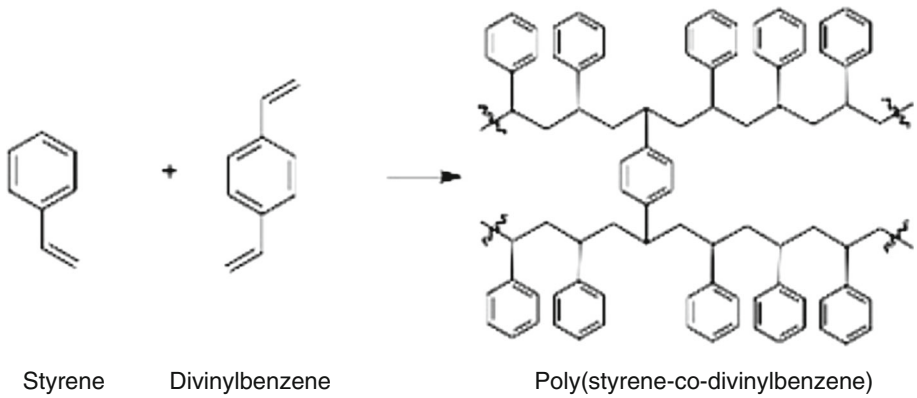


**Fig. 2** The reaction scheme of poly(styrene-co-divinylbenzene)

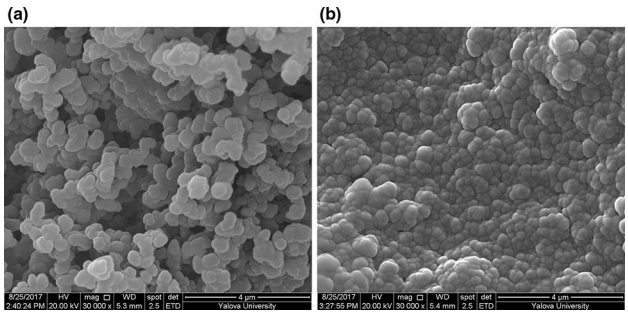


**Fig. 3** **a** SEM micrograph of the empty shell material and **b** SEM micrograph of the microencapsulated PCMs

$$\text{Microencapsulated PCM mixture (mass/\%)} = [\Delta H_{\text{microPCM}}/\Delta H_{\text{PCM mixture}}] \times 100 \quad (1)$$

Here, the mixture of $\Delta H_{\text{microPCM}}$ and $\Delta H_{\text{PCM}}$ refers to the enthalpies of the mixture of the microencapsulated PCM and pure PCM, respectively.

## Results and discussion

### Morphology and particle size distribution of microencapsulated PCMs

Encapsulation of the OA–CA–HD PCM mixture with St/DVB shell resulted in powdered product in white color. The morphology of microencapsulated PCM and the empty shell material are investigated using POM and SEM analyses. As seen in Fig. 3b, the results of encapsulation of the mixture of OA and CA fatty acids containing HD showed that the obtained microcapsules had a smooth surface and a nearly spherical appearance in a similar manner with the empty shell material (Fig. 3a).

The POM image of the PCM was obtained by dispersing the microparticles in water. In contrast to the empty shell material (Fig. 4a), the dark areas arising from the agglomeration of the microcapsules and the fact that the capsules are filled with PCM and therefore the light is not broken are clearly seen here (Fig. 4b). The average diameter of the obtained microcapsules was 0.304 ± 0.06 μm (304 ± 60 nm), and the particle size exhibited a narrow range between 0.20 and 0.50 μm (Fig. 5).

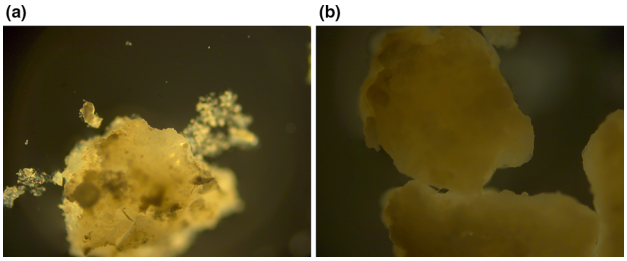


**Fig. 4** **a** POM image of the empty shell material and **b** POM image of the microencapsulated PCMs

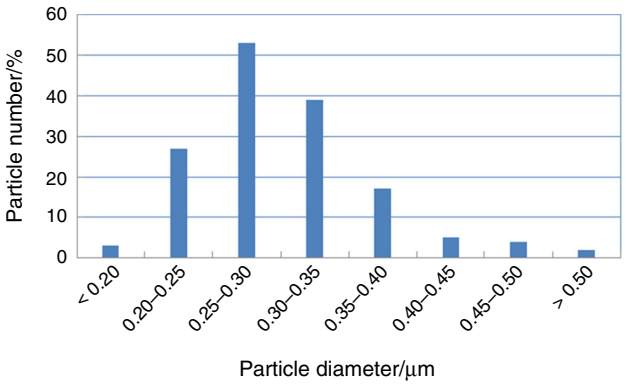


**Fig. 5** Particle size distribution of microencapsulated PCMs

### Chemical characterization of microencapsulated PCMs

FT-IR spectra of microencapsulated PCM, PCM mixture and shell material are given in Fig. 6. When the spectrum of the pure PCM mixture is examined, the absorbance

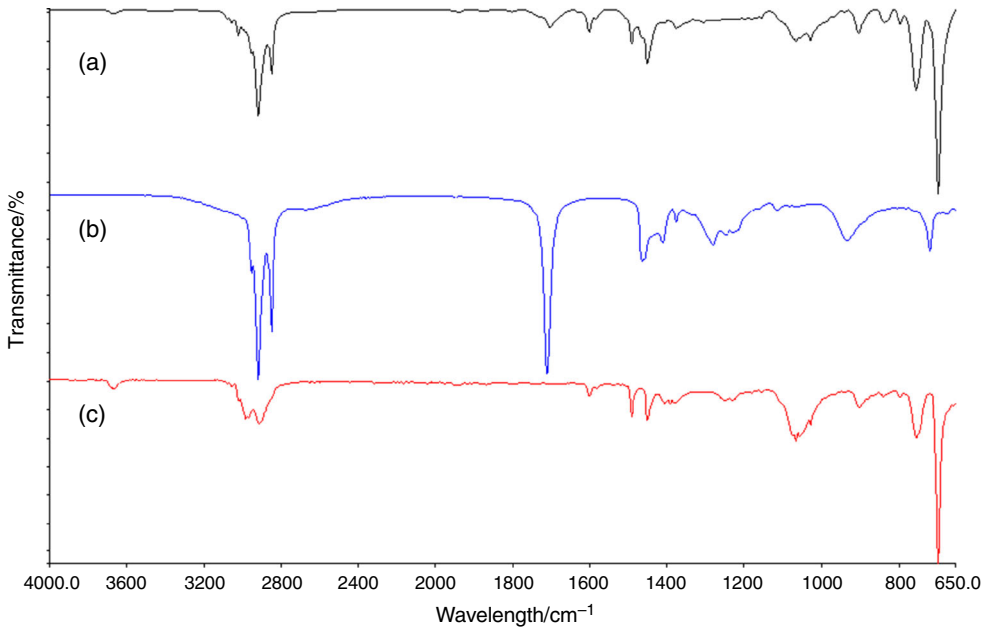


**Fig. 6** FT-IR spectra of (a) the microencapsulated PCMs, (b) mixture of PCMs and (c) shell material

bands at 2922 $cm^{-1}$ and 2853 $cm^{-1}$ are due to the stretching of aliphatic C–H groups. The characteristic band belonging to the C=O group of fatty acids is observed at 1709 $cm^{-1}$. As seen in the spectrum of the shell material, the bands of the characteristic aromatic C=C and C–H groups of the polystyrene are located at 1600–1450 $cm^{-1}$ and 750–700 $cm^{-1}$, respectively.

It is clearly seen from the FT-IR spectrum (Fig. 6a) that the characteristic peaks of pure PCM and shell material of the microencapsulated PCM confirm the encapsulation of the PCM mixture is successfully achieved.

## Thermal properties and latent heat storage capacities of microencapsulated PCMs

Figure 7a and b displays the melting and freezing DSC curves of the copolymer shell and microencapsulated PCM, respectively. As can be seen from Fig. 7b, the microencapsulated PCM melts at 24.0 °C and has a latent heat of fusion of 127.3 J $g^{-1}$ when regarding the heating curve. When the cooling curve was examined, it can be seen that the microcapsules crystallized at 14.1 °C and its latent heat of crystallization was − 128.5 J $g^{-1}$. The latent heat of fusion of the OA–CA–HD PCM mixture was also calculated according to the following formula [35] and it was found as 143.3 J $g^{-1}$ by using the latent heat of fusion of the pure components in Table 4.

$$\Delta H_{\mathrm{f,FDM\,mixture}} = (X_{\mathrm{OA}} \cdot \Delta H_{\mathrm{f,OA}}) + (X_{\mathrm{CA}} \cdot \Delta H_{\mathrm{f,CA}}) + (X_{\mathrm{HD}} \cdot \Delta H_{\mathrm{f,HD}}) \quad (2)$$

Here, $X_i$ is the mass fraction of pure i component in the PCM mixture and the $\Delta H_{f,i}$ is the latent heat of fusion of the pure component i (J $g^{-1}$).

Due to the presence of the polystyrene shell, the latent heat of the microencapsulated PCM (127.3 J $g^{-1}$) is expected to be lower than that of the pure OA–CA–HD PCM mixture (143.3 J $g^{-1}$).

The copolymer shell material did not show a peak due to the absence of core material (OA–CA–HD) (Fig. 7a). According to the results, the microencapsulated PCM was verified that it has a high thermal storage capacity. Moreover, the encapsulation ratio of the OA–CA–HD PCM mixture was also calculated as 88.8 (mass/%) according to Eq (1).

Thermal properties of the polystyrene shell, PCM mixture and microencapsulated PCM were determined by the TG method, and the results are given in Fig. 8 and Table 5. As it can be seen from the curves, the empty St–DVB copolymer shell degraded in a single step at a temperature range of 382.5–450.8 °C and lost 96.2% of its mass. Similarly, the PCM mixture degraded in a single step at a temperature range of 164.9–282.3 °C and lost 98.2% of its mass in this temperature range. In contrast, OA–CA–HD/St–DVB (1:1) microcapsules were degraded in two stages. The mass loss at the first stage was 67.8% which corresponds to the evaporation/decomposition of OA–CA–HD PCM mixture as the core material at the temperature range of 150.1–214.1 °C. At the second stage, the mass loss was determined as 28.4% that indicates the degradation of polystyrene shell at the temperature range of 377.8–455.6 °C. The data of the degradation of the materials are summarized in Table 5. When the degradation

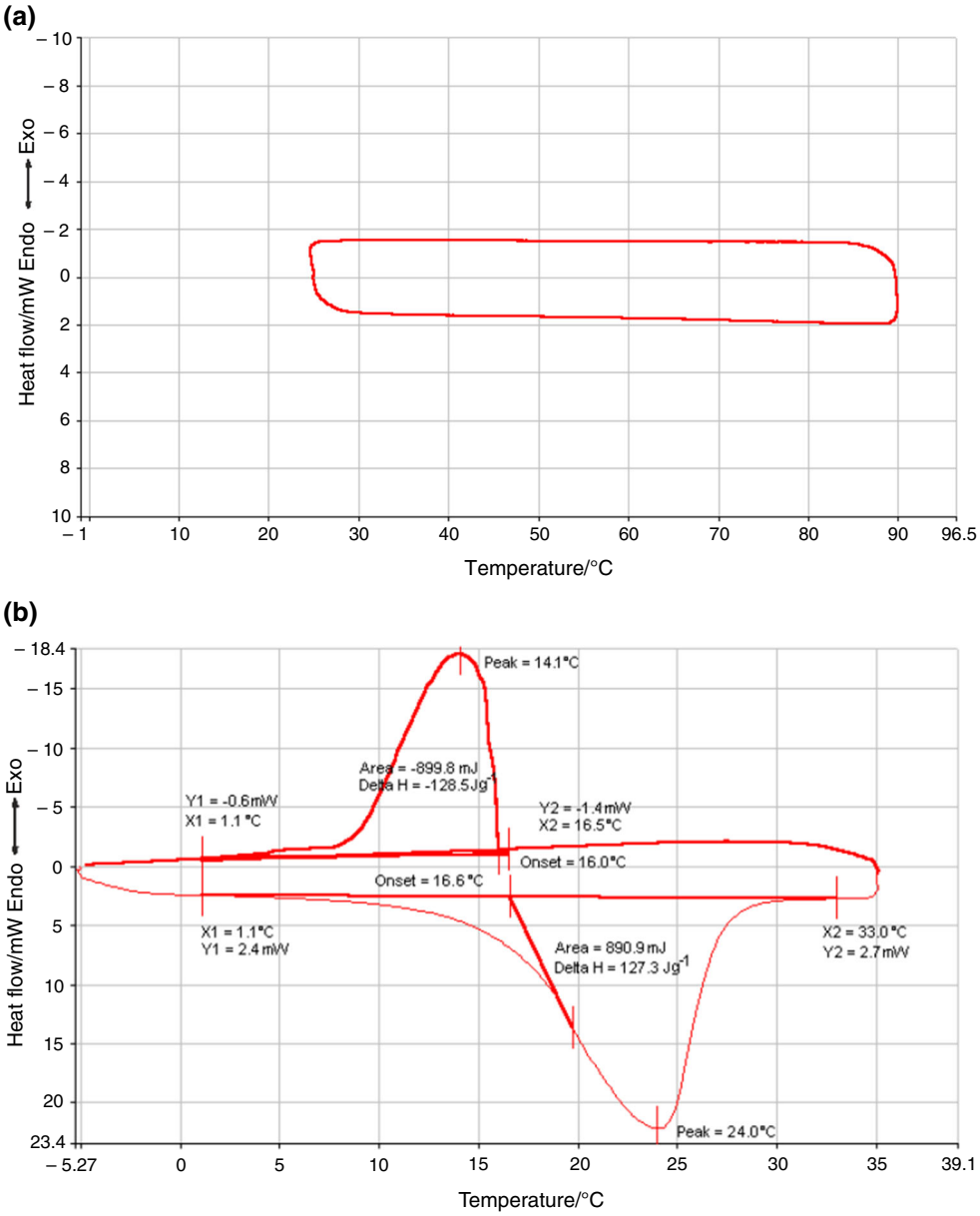


**Fig. 7** DSC curves of **a** copolymer shell and **b** the microencapsulated PCMs

**Table 4** Latent heats of fusion of the pure components of PCMs

| Pure component | $\Delta H_f$/J g$^{-1}$ |
|---|---|
| OA | 70.100[a] |
| CA | 133.232[b] |
| HD | 191.185[b] |

[a]Ref. [36]

[b]Determined by DSC analysis

temperatures of the second stage analyzed, it can be said that the prepared microcapsules and the empty copolymer shell show almost have the same thermal stability.

## Testing of heat storage property of the microencapsulated PCM

The heat storage property of the obtained PCM was examined using a laboratory scale experimental test system (Fig. 9) The system was consisted of a rectangular channel, a data acquisition system and a computer. The size of the channel is 149 × 119 × 691 mm, and its length is 700 mm. The channel includes a flat heating plate which was made of aluminum, and the size of the heating plate is 100 × 100 × 3 mm. Air was used as the heat-transfer fluid in the system, and it enters to the channel from 6 symmetrically distributed holes of 8 mm diameter on the left side of the test device. An air fan is located at the right

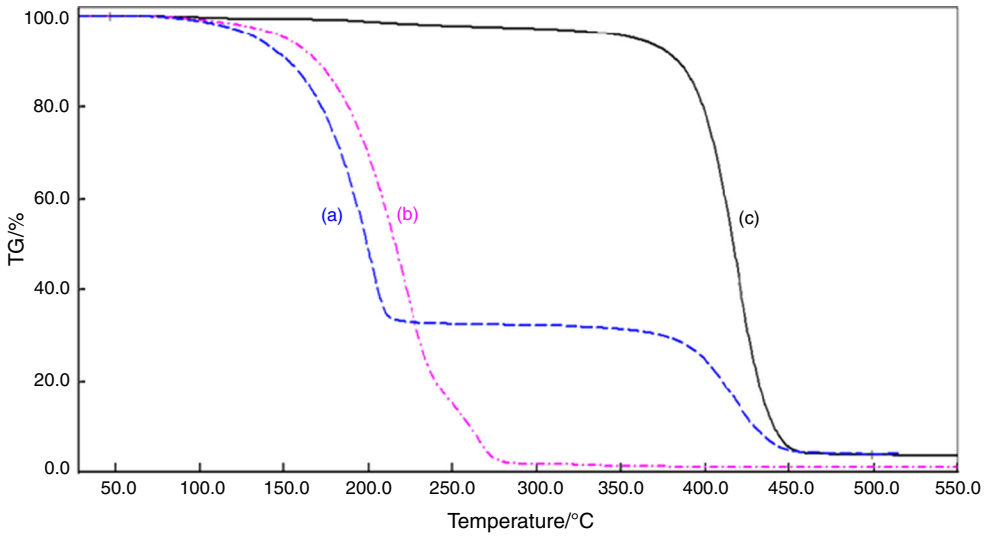


**Fig. 8** TG curves of (a) the microencapsulated PCMs, (b) mixture of PCMs and (c) shell material

**Table 5** TG/DTG results of PCMs, St–DVB copolymer shell and microencapsulated PCMs

| Sample no. | Samples | TG decomposition interval of stage-1/°C | DTG peak of stage-1/°C | Percent mass loss/% | Maximum rate of mass loss/% $min^{-1}$ | TG decomposition interval of stage-2/°C | DTG peak of stage-2/°C | Percent mass loss/% | Maximum rate of mass loss/%$min^{-1}$ |
|---|---|---|---|---|---|---|---|---|---|
| **1** | St/DVB copolymer shell | – | – | – | – | 382.5–450.8 | 418.9 | 96.2 | 21.28 |
| **2** | Microencapsulated PCM | 150.1–214.1 | 203.2 | 67.8 | 16.53 | 377.8–455.6 | 415.1 | 28.4 | 5.54 |
| **3** | Pure PCM mixture | 164.9–282.3 | 221.8 | 98.2 | 15.46 | – | – | – | – |

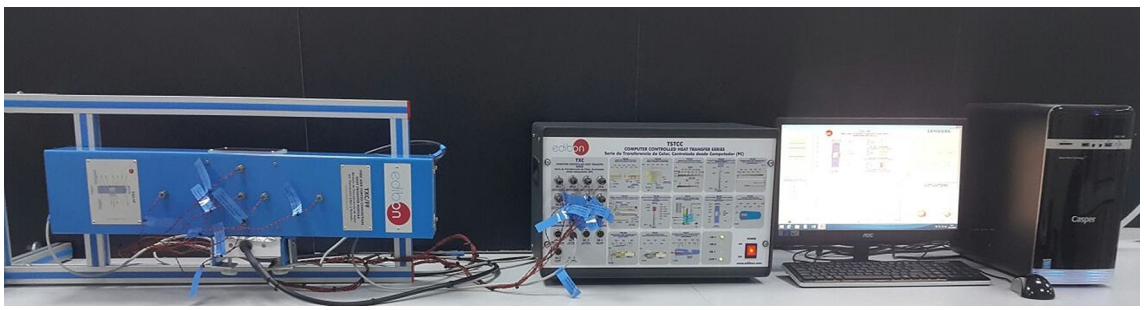

**Fig. 9** Test system

side of the channel to provide the required air flow and 8 J type thermocouples are mounted on the channel for experimental measurement. The heating plate is located in the middle bottom of the channel. The schematic diagram of the channel system is given in Fig. 10.

Data were collected with a data acquisition system. Here, ST-1 to ST-8 was the J type thermocouples; SC-1 was the air flow sensor; ST-CON was the temperature control element of the unit, and AR-1 was the power supply. All thermocouples were used to monitor instantaneous changes throughout the system. The data obtained from the thermocouples, namely the ST-5 and ST-8, which were located on the air channel nearest to the plate and in the heater plate, respectively, were examined and the heating–cooling curves were obtained.

In order to test the PCM's heat storage property, the experiments were conducted based on coating the heater plate with and without PCM. Figure 11a shows the side and top view of the heater plate, and Fig. 11b shows the

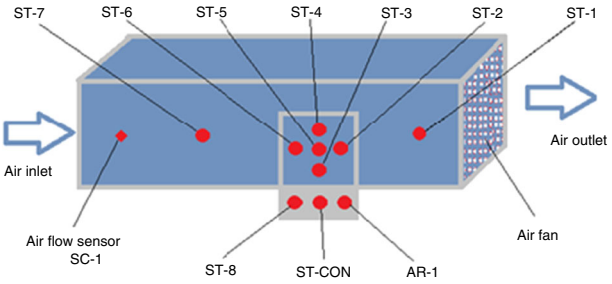


**Fig. 10** Schematic view of the channel

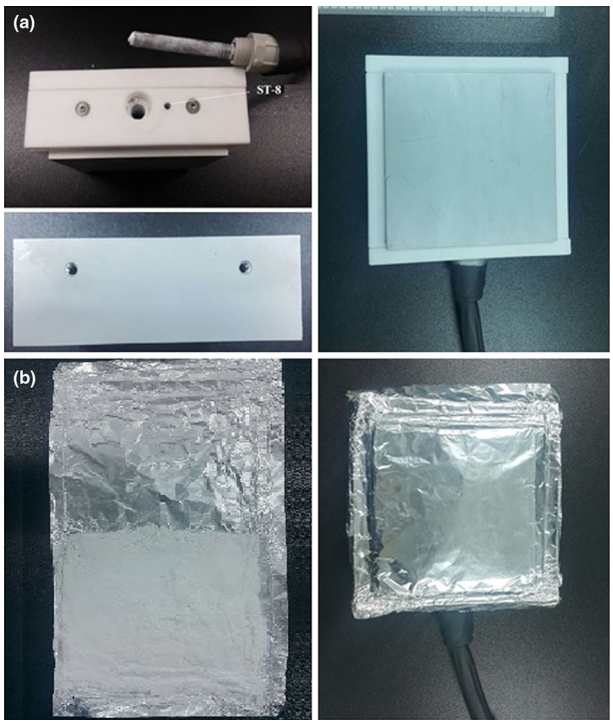


**Fig. 11** **a** The heater plate side and top views **b** powdered PCM and the PCM coated heater plate

powdered PCM and the PCM coated heater plate, respectively.

The experiments were carried out in similar conditions; the mass flow rate of the air and the power supplied to the system were constant. During the experiments, the room temperature and the relative humidity were also kept constant. Firstly, the air fan was operated at 100% fan load. Once the system reached to the steady-state condition, then the heating button was turned on. When the temperature of the heating plate reached to 44 °C, then the heating process terminated and the cooling process was observed while the fan was operating at 100% fan load.

Two distinctive experiments were performed on the test setup (Table 6). In the first experiment (D1), the blank aluminum foil without PCM was used to examine the effect of the foil on heat transfer. In the second experiment (D2), the heat storage property of the produced PCM was tested. The powdered PCM was placed in the aluminum foil, and the foil covered on the heater plate (Fig. 11b).

The data obtained from the ST-5 and ST-8 thermocouples were used to monitoring the temperature alterations in the system with and without PCM application. Figure 12 demonstrates the heating–cooling curves with and without PCM coating considering the temperature change of the air along *x*-axis parallel to the heated plate (ST5 was the closest thermocouple to the heated plate) and the temperature change of the heated plate (ST8).

The effect of PCM coating and the heat storage property of the PCM can be clearly observed from Fig. 12. During the experimental investigation, the heating of the plate was switched on for the heating process when the steady-state conditions achieved. In the heating process, it was obvious that the heated plate reached to 44 °C in the absence of PCM much earlier than that of operation with PCM coating. A part of the heat that was given to the plate was stored by the PCM. Thus, it took longer for the plate to reach 44 °C.

After that the heating was switched off; the PCM attempted to maintain its current heat, and this was caused the temperature of the plate to fall faster in the cooling process. On the other hand, the temperature change of the air was observed by the thermocouple-ST5 which was closest to the heated plate. The temperature of the air flowing over the heated plate remained almost constant with the PCM coating due to its heat storage property in both the heating and cooling processes. However, in the operation without PCM coating, the measured air temperature was first increased and then decreased in an observable manner with the temperature change of the plate.

**Table 6** Features of the tested PCM in the experiments

| Experiment number | PCM | Latent heat of fusion/kJ $kg^{-1}$ | Melting temperature/°C |
|---|---|---|---|
| D1 | No | – | – |
| D2 | Yes | 127.3 | 24.0 |

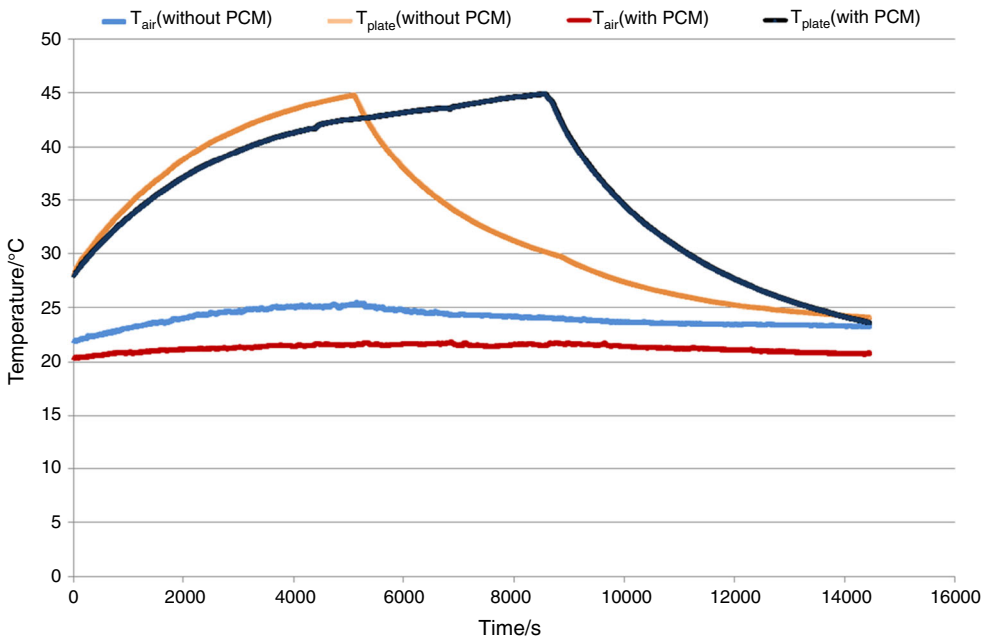


**Fig. 12** Heating and cooling curves considering the temperature change of the air and the temperature change of the heated plate with and without PCM coating

## Conclusions

In this study, microencapsulated PCM consisting of OA–CA–HD mixture as the core and polystyrene as the shell was successfully synthesized by emulsion polymerization technique. The encapsulation ratio was found to be 88.8%, and the properties of microencapsulated PCM were clarified by FT-IR, TG, SEM and POM analyzes. The resulting microcapsules exhibited a homogeneous size distribution ranging from 0.20 to 0.50 μm and were obtained in almost spherical morphology.

The results obtained from the DSC analysis show that the microencapsulated OA–CA–HD mixture is a good PCM candidate for low-temperature thermal energy storage applications with its appropriate temperature range (14.1–24.0 °C) and latent heat of fusion (127.3 J $g^{-1}$). Therefore, the heat storage property of the produced PCM was tested in an experimental system at laboratory scale. The testing of the PCM was conducted with the operation with and without PCM coating, and the test was verified that the obtained PCM has the heat storage features.

Thermal energy storage technologies can provide effective use of resources and reduce total energy consumption of the systems. The phase change materials (PCMs) are the good candidates for achieving this goal. PCMs can also be seen as one of the promising choices for to reduce the discrepancy between energy production and consumption. It is possible to use PCMs in heating and cooling systems, electronic equipment cooling applications, as well as construction materials in buildings. The obtained microencapsulated PCM consisting of OA–CA–HD in this work has appropriate phase change temperature and can be used in various low-temperature thermal systems for energy-saving applications, especially in air conditioning and refrigeration systems. Moreover, it can also be safely stated that OA–CA–HD/St–DVB microcapsules may serve like a smart material for thermal regulation of some parts of the building by impregnation of microcapsules into construction materials.

**Acknowledgements** The authors appreciate the support of Research Fund of Yalova University (Project Number: 2017/YL/008) for the accomplishment of this work. Authors thank Dr. Ali Karaipekli (Çankırı Karatekin University, Turkey) for DSC analyses.

## References

1. Farid MM, Khudhair AM, Razack SAK, Al-Hallaj S. A review on phase change energy storage: materials and applications. Energy Convers Manag. 2004;45:1597–615.
2. Rozanna D, Chuah TG, Salmiah A, Choong TSY, Sa'ari M. Fatty acids as phase change materials (PCMs) for thermal energy storage: a review. Int J Green Energy. 2004;1:495–513.
3. Baetens R, Jelle BP, Gustavsen A. Phase change materials for building applications: a state-of-the-art review. Energy Build. 2010;42:1361–8.
4. Su W, Darkwa J, Kokogiannakis G. Review of solid–liquid phase change materials and their encapsulation technologies. Renew Sustain Energy Rev. 2015;48:373–91.
5. Sarı A, Alkan C, Karaipekli A. Preparation, characterization and thermal properties of PMMA/*n*-heptadecane microcapsules as novel solid–liquid microPCM for thermal energy storage. Appl Energy. 2010;87(5):1529–34.
6. Alay S, Alkan C, Göde F. Synthesis and characterization of poly(methyl methacrylate)/*n*-hexadecane microcapsules using different cross-linkers and their application to some fabrics. Thermochim Acta. 2011;518(1–2):1–8.

7. Tumirah K, Hussein MZ, Zulkarnain Z, Rafeadah R. Nano-encapsulated organic phase change material based on copolymer nanocomposites for thermal energy storage. Energy. 2014;66:881–90.
8. Jiang X, Luo R, Peng F, Fang Y, Akiyama T, Wang S. Synthesis, characterization and thermal properties of paraffin microcapsules modified with nano-Al2O3. Appl Energy. 2015;137:731–7.
9. Li M, Wu Z. Thermal properties of the graphite/*n*-docosane composite PCM. J Therm Anal Calorim. 2013;111:77–83.
10. Xia Y, Cui W, Zhang H, Zou Y, Xiang C, Chu H, Qiu S, Xu F, Sun L. Preparation and thermal performance of *n*-octadecane/expanded graphite composite phase-change materials for thermal management. J Therm Anal Calorim. 2018;131:81–8.
11. Genc M, Karagoz-Genc Z. Microencapsulated myristic acid–fly ash with $TiO_2$ shell as a novel phase change material for building application. J Therm Anal Calorim. 2018;131:2373–80.
12. Meng X, Zhang H, Sun L, Xu F, Jiao Q, Zhao Z, Zhang J, Zhou H, Sawada Y, Liu Y. Preparation and thermal properties of fatty acids/CNTs composite as shape-stabilized phase change materials. J Therm Anal Calorim. 2013;111:377–84.
13. Alkan C, Sarı A. Fatty acid/poly(methyl methacrylate) (PMMA) blends as form stable phase change materials for latent heat thermal energy storage. Sol Energy. 2008;82:118–24.
14. Sarı A, Alkan C, Karaipekli A, Önal A. Preparation, characterization and thermal properties of styrene maleic anhydride copolymer (SMA)/fatty acid composites as form stable phase change materials. Energy Convers Manag. 2008;49(2):373–80.
15. Bellemare JV. Thermally reflective encapsulated phase change pigment, United States Patent office. 2007; No. 0031652 A1.
16. Zhang X, Chao N, Zhang X, Xu J. Natural microtubule encapsulated phase- change materials and preparation thereof, United States Patent office. 2010; No. 0071882A1.
17. Hart RL, Work DE Flame resistant microencapsulated phase change materials, United States Patent office. 1995; No. 5, 435,376.
18. Hatfield JC. Encapsulation of phase change materials, United States Patent office. 1987; No. 4, 708,812.
19. Yuan Y, Zhang N, Tao W, Cao X, He Y. Fatty acids as phase change materials: a review. Renew Sustain Energy Rev. 2014;29:482–98.
20. Ke H. Phase diagrams, eutectic mass ratios and thermal energy storage properties of multiple fatty acid eutectics as novel solid–liquid phase change materials for storage and retrieval of thermal energy. Appl Therm Eng. 2017;113:1319–31.
21. Sharma A, Shukla A, Chen CR, Wu TN. Development of phase change materials (PCMs) for low temperature energy storage applications. Sustain Energy Technol Assess. 2014;7:17–21.
22. Karaipekli A, Sarı A. Capric–myristic acid/expanded perlite composite as form-stable phase change material for latent heat thermal energy storage. Renew Energy. 2008;33:2599–605.
23. Karaipekli A, Sarı A. Preparation, thermal properties and thermal reliability of eutectic mixtures of fatty acids/expanded vermiculite as novel form-stable composites for energy storage. J Ind Eng Chem. 2010;16:767–73.
24. Sarı A, Sarı H, Önal A. Thermal properties and thermal reliability of eutectic mixtures of some fatty acids as latent heat storage materials. Energy Convers Manag. 2004;45:365–76.
25. Sarı A. Eutectic mixtures of some fatty acids for low temperature solar heating applications: thermal properties and thermal reliability. Appl Therm Eng. 2005;25:2100–7.
26. Sari A. Eutectic mixtures of some fatty acids for latent heat storage: thermal properties and thermal reliability with respect to thermal cycling. Energy Convers Manag. 2006;47:1207–21.
27. Yang X, Yuan Y, Zhang N, Cao X, Liu C. Preparation and properties of myristic–palmitic–stearic acid/expanded graphite composites as phase change materials for energy storage. Sol Energy. 2014;99:259–66.
28. Inoue T, Hisatsugu Y, Ishikawa R, Suzuki M. Solid-liquid phase behavior of binary fatty acid mixtures 2. Mixtures of oleic acid with lauric acid, myristic acid, and palmitic acid. Chem Phys Lipids. 2004;127:161–73.
29. Zhang H, Gao X, Chen C, Xu T, Fang Y, Zhang Z. A capric–palmitic–stearic acid ternary eutectic mixture/expanded graphite composite phase change material for thermal energy storage. Compos Part A Appl S. 2016;87:138–45.
30. Liu C, Yuan Y, Zhang N, Cao X, Yang X. A novel PCM of lauric–myristic–stearic acid/expanded graphite composite for thermal energy storage. Mater Lett. 2014;120:43–6.
31. Zhang N, Yuan Y, Wang X, Cao X, Yang X, Hu S. Preparation and characterization of lauric–myristic–palmitic acid ternary eutectic mixtures/expanded graphite composite phase change material for thermal energy storage. Chem Eng J. 2013;231:214–9.
32. Schork FJ, Luo Y, Smulders W, Russum JP, Butté A, Fontenot K. Miniemulsion polymerization. In: Okubo M, editor. Polymer particles. Advances in polymer science, vol. 175. Berlin: Springer; 2005. p. 129–255.
33. Azad ARM, Ugelstad J, Fitch RM, Hansen FK. Emulsification and emulsion polymerization of styrene using mixtures of cationic surfactant and long chain fatty alcohols or alkanes as emulsifiers. ACS Symp Ser. 1976;24(1):1–23.
34. Sari A, Alkan C, Döğüşcü DK, Kızıl Ç. Micro/nano encapsulated *n*-tetracosane and *n*-octadecane eutectic mixture with polystyrene shell for low-temperature latent heat thermal energy storage applications. Sol Energy. 2015;115:195–203.
35. Meltzer V, Pincu E. Thermodynamic study of binary mixture of citric acid and tartaric acid. Cent Eur J Chem. 2012;10(5):1584–9.
36. Beyhan B, Paksoy H, Daşgan Y. Root zone temperature control with thermal energy storage in phase change materials for soilless greenhouse applications. Energy Convers Manag. 2013;74:446–53.